Estimating density of mountain hares using distance sampling: a comparison of daylight visual surveys, night-time thermal imaging and camera traps

Authors: Bedson, Carlos P. E., Thomas, Lowri, Wheeler, Philip M., Reid, Neil, Harris, W. Edwin, et al.

Estimating density of mountain hares using distance sampling: a comparison of daylight visual surveys, night-time thermal imaging and camera traps

Carlos P. E. Bedson, Lowri Thomas, Philip M. Wheeler, Neil Reid, W. Edwin Harris, Huw Lloyd, David Mallon and Richard Preziosi

C. P. E. Bedson (https://orcid.org/0000-0001-6489-1138) ✉ (carlosbedson@outlook.com), H. Lloyd, D. Mallon and R. Preziosi, Dept of Natural Sciences, Manchester Metropolitan Univ., UK. – L. Thomas, Faculty of Biology, Medicine and Health, Univ. of Manchester, UK. – P. M. Wheeler, School of Environment, Earth and Ecosystem Sciences, The Open Univ., Milton Keynes, UK. – N. Reid, Inst. of Global Food Security (IGFS), School of Biological Sciences, Queen's Univ. Belfast, Belfast, Northern Ireland, UK. – W. E. Harris, Dept of Agriculture and Environment, Harper Adams Univ., Newport, Shropshire, UK.

Surveying cryptic, nocturnal animals is logistically challenging. Consequently, density estimates may be imprecise and uncertain. Survey innovations mitigate ecological and observational difficulties contributing to estimation variance. Thus, comparisons of survey techniques are critical to evaluate estimates of abundance. We simultaneously compared three methods for observing mountain hare *Lepus timidus* using Distance sampling to estimate abundance. Daylight visual surveys achieved 41 detections, estimating density at 14.3 hares km^{-2} (95%CI 6.3–32.5) resulting in the lowest estimate and widest confidence interval. Night-time thermal imaging achieved 206 detections, estimating density at 12.1 hares km^{-2} (95%CI 7.6–19.4). Thermal imaging captured more observations at furthest distances, and detected larger group sizes. Camera traps achieved 3705 night-time detections, estimating density at 22.6 hares km^{-2} (95%CI 17.1–29.9). Between the methods, detections were spatially correlated, although the estimates of density varied. Our results suggest that daylight visual surveys tended to underestimate density, failing to reflect nocturnal activity. Thermal imaging captured nocturnal activity, providing a higher detection rate, but required fine weather. Camera traps captured nocturnal activity, and operated 24/7 throughout harsh weather, but needed careful consideration of empirical assumptions. We discuss the merits and limitations of each method with respect to the estimation of population density in the field.

Keywords: camera traps, cryptic animals, distance sampling, population monitoring, survey methods, thermal imager, uplands

In a global era of biodiversity crisis, conservation monitoring which allows us to establish trends in wild animal abundance, is essential. The provision of reliable census estimates are considered vital to guide management interventions aimed at protecting vulnerable species (Krebs 1989). Effective surveys must be designed to reflect species distribution and life history traits which may affect animal detection. Studies must comprise sites which represent the range of habitats, climate and topography occupied by the target species and this will both inform and constrain survey methods (Sutherland 2006).

The mountain hare *Lepus timidus* is Britain's only native lagomorph and an icon for upland habitats and their con-servation. Reliable estimates of mountain hare population density are important to inform conservation assessments and to evaluate the impact of anthropogenic disturbance on population numbers (e.g. impact of roadkill or control efforts on grouse moorland). Yet hares are mostly nocturnal mammals and can be difficult to detect (Newey et al. 2011, Petrovan et al. 2011). Despite having a white pelage in winter, hares are adept at hiding by day in rough vegetation: they lie motionless, flattening to 15 cm height, sometimes in shallow depressions, burrows or amongst rocks and even fleeing unseen. Hares emerge at night to feed (Hewson and Hinge 1990, Harris and Yalden 2008) and consequently daytime observation is characterised by low detection rates (Dingerkus and Montgomery 2002).

Surveying elusive or nocturnal animals is particularly challenging in environments such as upland terrains which often experience poor weather. Mountain hare habitats are also frequently rugose and difficult to access, creating safety issues for monitoring, especially at night. Mountain hares

frequent low hills, gullies and deep vegetation, making detection difficult (Newey et al. 2018). Snow may hamper daytime observations of white camouflaged mountain hares. Effective monitoring therefore requires multiple observation points and benign weather.

Considering the suite of study methods available for wildlife monitoring, mark–recapture is regarded as the most reliable for hares (Boulanger and Krebs 1994). However, addressing welfare concerns surrounding the capture and handling of animals is resource intensive, particularly in rough terrain, making this method expensive and impractical. Faecal pellet counts can provide a useful index in areas of high hare density, assuming constant accumulation rates (Newey et al. 2003). Whilst it is also possible to obtain DNA from faecal pellets for genetic population monitoring with molecular mark–recapture, both plant material in the pellets and fast decay rates can reduce PCR effectiveness, requiring larger sample sizes and greater field and laboratory work and costs (DeMay et al. 2013). Direct observation methods by day, such as line transect sampling, are commonly used yet are vulnerable to achieving fewer observations when such predominantly nocturnal animals remain undetected (Buckland et al. 2001). Areas of low density may result in low encounter rates and wide variance in estimates (Newey et al. 2018). Night-time spotlight surveys may miss animals as they rely on eyeshine reflections, and frequently sample along roads which animals may avoid and which locations represent only a small fraction of upland habitat (Reid et al. 2007, Reid and Montgomery 2010). Thermal imaging reduces false negatives by increasing target detections, contrasting body heat against a cold backdrop at night (Havens and Sharp 2016) but if the aim is to estimate density it also requires a means to determine distance to the object in darkness. Camera trapping provides a greater continuous survey effort including during night peak activity periods thus increasing total numbers of detections (Caravaggi et al. 2018), and with virtually no observer field presence to disturb animals (Sollman 2018).

In this study we compared three survey methods of mountain hares in upland habitat to estimate density and considered factors relating to spatial variation of hare detections: 1) daylight visual surveys, 2) night-time thermal imaging point transects and 3) fixed position camera traps. We analysed data from each method using comparable distance sampling models to estimate density and associated precision. For each method we recorded survey effort, observations, distances to target animals and group sizes as inputs to estimate density. As camera trap distance sampling methods are relatively recent, we also explored how different assumptions of space, time and animal behaviour affected density estimates. Since actual densities or population size were not known, we could not be certain which density estimate of the three methods might be closest to the truth. Nonetheless the overall precision of parameters and estimates could be compared. We compared variation of estimates among methods and survey sites, the effect of terrain type and how detection rates changed throughout the study period. We evaluate the merits and assumptions of each method relative to our findings, to inform study design decisions for conservation monitoring.

Methods and materials

Study site

Surveys took place at Holme Moss, a large hill, elevation 582 m a.s.l., situated in the north of England, UK (Fig. 1). Mountain hares were once native to England yet became extinct ~ 6000 years ago (Yalden 1971). They were reintroduced to Holme Moss in the 1870s for sport shooting (Stubbs 1929, Yalden 1971). In this area historic records suggest the number of 1-km squares occupied by mountain hares as ranging from 16 (Yalden 1971) up to 35 (Mallon et al. 2003). This group of hares is potentially partially isolated from other populations elsewhere in the area by reservoir systems and major road networks. Whilst sightings of mountain hares on Holme Moss have been particularly frequent in the past (Mallon et al. 2003), farmers and landowners report perceived declines across the site in the last decade. The local density on Holme Moss has never been formally quantified. Holme Moss comprises a flat plateau with peat gullies and steep sided valleys (Fig. 1) (Tallis 1987). The area consists of blanket bog vegetation dominated by heather *Calluna vulgaris*, bilberry *Vaccinium myrtillis* and cotton grass *Eriphorum* spp. Over the last 200 years habitat conditions have deteriorated as both acid rain caused peat layer reduction and intensive sheep grazing led to widespread vegetation loss (Anderson and Shimwell 1981). Most of the hill is managed by the RSPB Dove Stone reserve engaged in blanket bog restoration.

The study focused on the entire blanket bog plateau of Holme Moss, where elevation was above 335 m i.e. the lower elevation range of mountain hare occurrence (Yalden 1971), and as limited by major roads to the north and east and different habitats to the south and west. This comprised 49 km². Within this area we selected a smaller 5 × 5 km central area for daylight visual surveys, thermal imager and camera trap surveys. This considered the area that could be covered on foot by two full time staff conducting field logistics: Holme Moss is largely pathless, often hazardous underfoot. Winter day lengths are short. The location of the 5 × 5 km area was chosen to be central, equidistant from roads and habitat edges, avoiding edge areas frequented by the public, thereby reducing camera theft risk, though accepting this choice of centroid might cause bias. Within this area we then randomly selected (R-package 'sample') 5 × 5 1-km squares as the locations for random cluster samples of points and transects, being representative of the flat blanket bog. The location of an additional sixth site was also randomly selected, yet at the request of wildlife agencies we altered its shape to comprise a narrow long strip to facilitate monitoring of an historic high density area (Mallon et al. 2003), accepting this might bias results. Contemporary density and distribution of hares was unknown. The 1-km size of each study site enabled comprehensive continuous observation of terrain, detecting potential changes in hare occurrence over a few hundred metres. Hare home ranges can be small (0.1–0.8 km²), non-territorial, overlapping and hares sometimes group together (Hewson and Hinge 1990, Hulbert et al. 1996, Rao et al. 2003, Harrison 2011). The small 1-km site scale facilitated efficient management of camera arrays and enabled observers to learn of local topography and
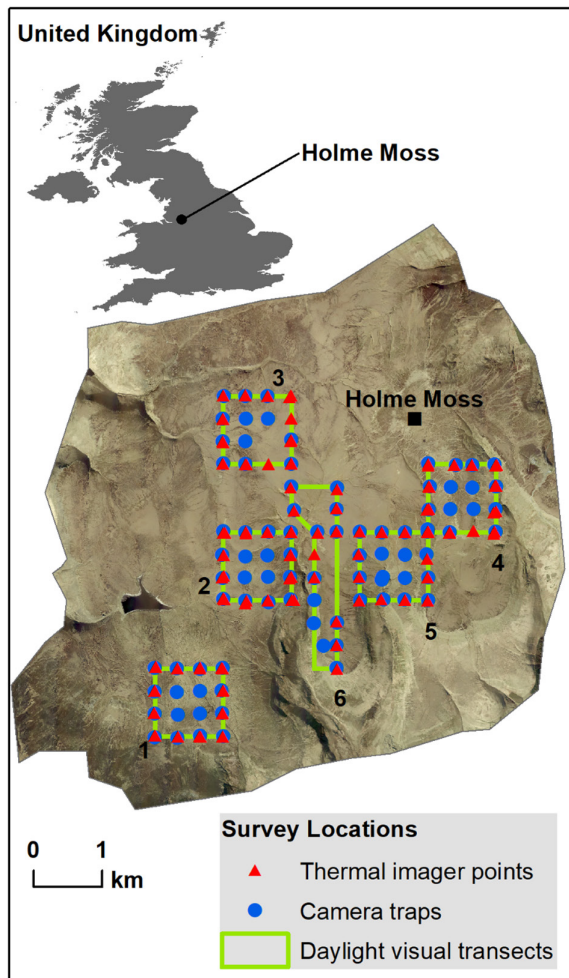
Figure 1. Location of Holme Moss study site, north west England, Great Britain. Aerial photo origin is OS SE 401398 and shows extent of Holme Moss massif, above 335 m elevation, bounded to north and east by major roads. The hill summit is indicated by the black square. Survey locations are shown, with site numbers. Sites 1–5 are 1 km squares. Site 6 is the narrow polygon running north to south between sites 2 and 5. Daylight visual transects were the perimeter of 1-km square, except site 6 being a near trapezoid shape. Thermal imager points were 333 m apart as were camera traps, though with some minor deviations for topography, standing water or perceived theft risk. Note: one thermal imager point was used in site 4 and repeated ~30 m away in site 5; 87 of 91 camera site locations are shown as 4 pairs of camera trap sites overlap; 2 were moved ~30 m mid-term because of rising standing water; 2 were moved ~30 m avoiding perceived theft risk. Three cameras were stolen from site 3 and one from site 6; their points are not shown, no data was recorded at those locations. Aerial photograph: Digimap sourced June 2019 from Digimap Ordnance Survey Collection: Getmapping aerial imagery.

hazards, prior to subsequent night surveys for thermal imaging. Within the six study sites, we chose transect and point layouts which would cover the same locations, to capture the same local variation. However some of the survey locations between methods differed slightly to account for the different observation ranges of equipment. Surveys occurred from November 2017 to May 2018 (Supporting information). The period was characterised by exceptionally severe weather including seven heavy snowfalls (UK Met Office 2019).

Daylight visual surveys

Daylight visual surveys took place using line transects following Ordnance Survey (2015) Explorer Map 1 grid lines which bounded each survey site (Fig. 1). Transects were square circuits (Buckland et al. 2001, p. 237), intended to alleviate detection bias arising from a low winter sun position when walking different cardinal directions, wind or local topography effects, whilst enabling efficient use of survey time. Whilst surveys were conducted only during good visibility, poor weather and persistent snow cover limited the survey opportunities to only one visit per site transect. Observer routes were guided by a handheld GPS. A slow, measured walk was used (~ 1 km per hour), with frequent scanning of the landscape using binoculars (Fig. 2). The location of each mountain hare was recorded, measuring radial distance from the observer with a laser range finder (maximum range 1100 m) and angle using a compass. These measurements allowed the calculation of the perpendicular distance of sightings from the line, and also enabled the location of each hare to be mapped. During these surveys, conducted when there was no snow, mountain hares bore white pelage contrasting against the green and brown moorland. Hares were often lying-up and not detected until within 30 m range (Fig. 2). Whilst some hares fled from the observer, this occurred within the range of vision, so distance and angles were measured to point of origin.

Night-time thermal imaging

We conducted nocturnal surveys at point transect locations using an Armasight Command 336 HD 30 Hz 75 mm biocular (two view lenses) thermal camera, with a range of 2 km, and a refresh rate 30 Hz which enabled species identification of moving animals (Fig. 2). The camera was fitted with an Advanced Modular Range Finder 2200 which operated in darkness. In trials, distances up to 1.8 km could be measured. This assemblage was mounted on a tripod at each point location each spaced ~333 m apart (about the diameter of a single hare home range) along the same 1-km grid lines used during daylight visual surveys (Fig. 1). Thus, whilst a different survey method was used at a different time of day, survey sites were the same. Surveys did not occur at a location that had received a visit that day for other survey purposes, to ensure hares had not been disturbed. Points at sites 1–4 were visited 2–3 times over the winter; points at sites 5 and 6 were visited once only.

Surveys were conducted one hour after sunset with clear visibility though some surveys were curtailed by fog or high winds. Some surveys occurred on snow which assisted detection of hares. Walking by night from point to point took approximately 20–30 min. A red-light head-torch was used by observers to guide the way between points, minimising disturbance. Hares were seen twice only during transit. Once set up, the thermal imager assemblage was immobile; care was taken to situate it with the best field of view within 20 m of the GPS point. Whilst setting up the thermal imager vantage point no hares were observed within 30 m. Surveys at each point transect consisted of complete 360° field scans and typically took 10–20 min per point. Extensive practice with the thermal imager using the setting 'white hot' ensured
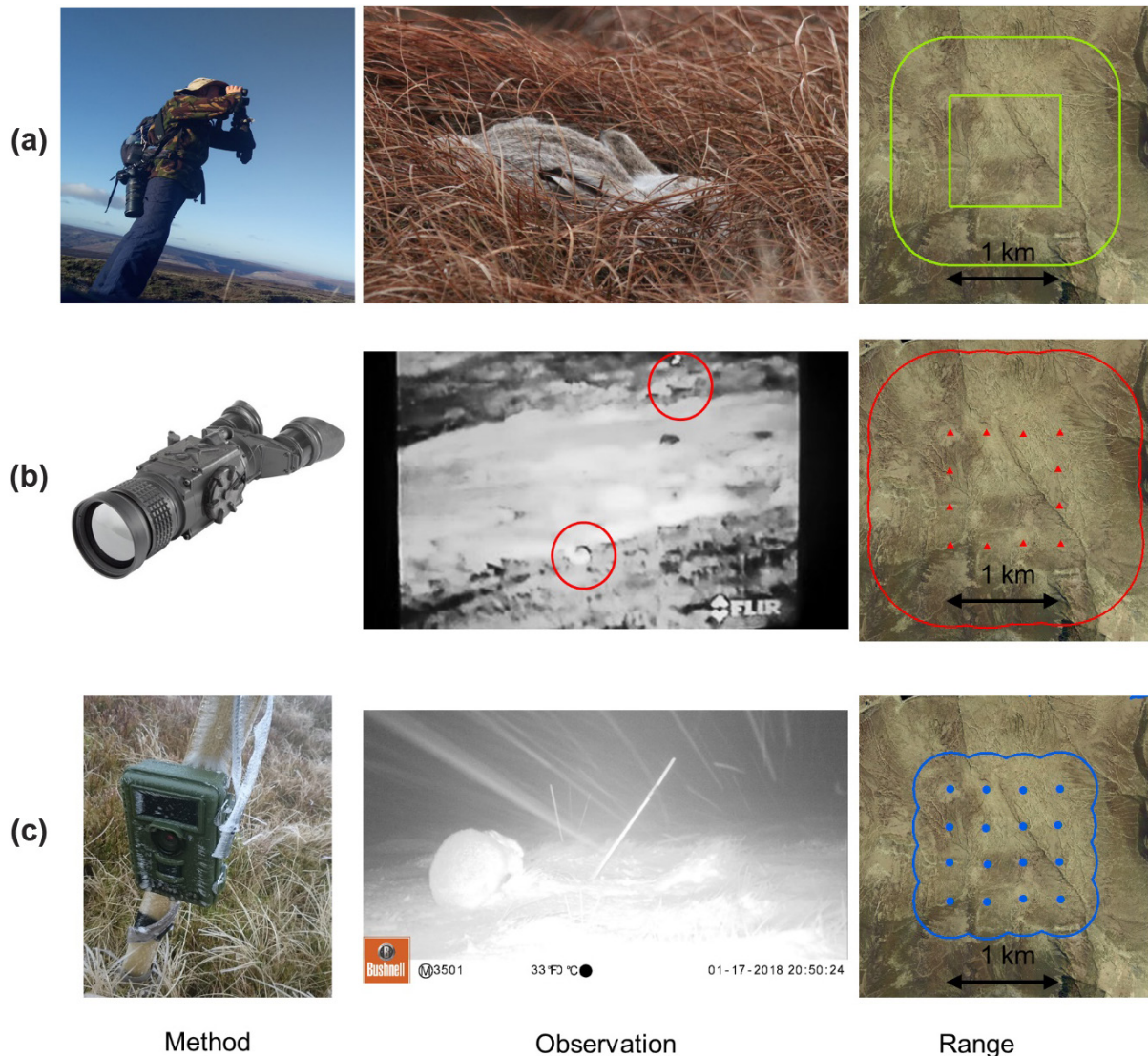
Figure 2. Photographs showing the three different methods. (a) Daylight visual surveys, (b) thermal imager, (c) camera trap. Left column shows the observation equipment. Central column shows each method's typical sighting of a mountain hare. Right hand column displays example survey location at site 1 for each method, duly surrounded by a buffer: measured to the furthest visual point (532 m) for daylight visual surveys; (740 m) thermal imager; for camera traps, buffer is portrayed to 333 m of each camera, the assumed home range of local mountain hares.

identification of hares which were easily distinguished from grouse *Lagopus lagopus* whose feathers blocked heat radiation except for beaks, and foxes *Vulpes vulpes* that were much larger (Fig. 2). For each detection, angle and distance measurements were recorded as during daylight surveys. Three sightings of leverets were excluded, to estimate adult densities only.

Camera traps

We placed between 12 and 16 camera traps at each of the six survey sites (Fig. 1). Due to logistical constraints, camera traps were deployed at site 1 before being moved sequentially to site 6 (they could not be deployed simultaneously). Cameras were left in situ for two to five weeks at each site (Supporting information), depending on weather conditions, camera performance and perceived risk of theft. Cameras were sited at the same locations as daylight visual surveys and thermal imaging surveys, along the Ordnance Survey map bounding grid lines of each site as well as several placed in the centre of each square for fuller coverage. Distances between cameras were thus 333 m, again this being the assumed home range diameter of mountain hares. Cameras were 14 MP Bushnell NatureView No Glow, set to high sensitivity. Pilot tests showed a large number of false detections would be elicited (wind blown vegetation). Capturing video might expend battery and memory capacity before revisits by staff and also make image review time excessive. Thus cameras were instead set to trigger at 1 s intervals with time-stamp recording. Camera functioning was evidenced by a 12 hourly 'field scan' setting. Cameras were installed on posts at 40 cm above ground level (Fig. 2) set facing north to avoid false triggers by sun movements. Bamboo canes were placed in a line at intervals of 2, 4, 6, 8 and 10 m in front of each

camera to measure the distance of each hare to the camera at 1 m spacing (Fig. 2) (Hofmeester et al. 2016, Howe et al. 2017). Photos were managed with TIMELAPSE 2 (University of Calgary, Canada) software. Images were catalogued by location, date and time.

We reviewed the frequency of camera images of hares and considered one second as representing the survey snapshot period ('k') for point counts following advice from Howe et al. (2017) to use time periods < 3 s. For each positive detection we recorded each individual's radial distance to camera for distance sampling estimation. In a few cases with darkness or poor focus this was difficult to determine. Images showed some hares, having appeared in the camera zone, inspected the distance marker cane or the camera itself. We considered this attraction behaviour, known to contribute to sampling bias (Corlatti et al. 2020) and discounted those images.

Unlike daylight visual surveys and night-time thermal imaging where surveys were time limited, camera traps can make detections 24/7. No detections are likely to be made when an animal is resting and so survey effort during daylight is highly vulnerable to false negatives, potentially lowering average density estimates. We defined the hare activity cycle using a frequency histogram of detections against each hour of the 24-h cycle, fitting a smoothed density function for each site according to standard methods (Ridout and Linkie 2009, Rowcliffe 2014). Conservative approaches may consider analysis which refers to the peak diel periods when ~ 50% of activity occurs (Frey et al. 2017) or ≥ 55% activity (McGowan et al. 2019). However our camera sites occurred over four months, winter solstice to spring equinox, when nights became shorter. Thus when assessing the activity frequency densities and potential correlations between sites with R-package 'overlap' (Meredith and Ridout 2020) we found different timings of bimodal activity patterns. For consistency we therefore defined the night-time period as sunset-to-sunrise at the mid-term date per site (HM Nautical Almanac Office 2019) thought to provide accurate levels of activity (Vazquez et al. 2019). This night-time period encompassed > 95% of all camera trap detections.

Distance sampling

Data from each method were analysed using software distance ver. 7.2 (Thomas et al. 2010) including site, survey effort, number of detections, distance to each detection and cluster size (Buckland et al. 2001).

Daylight visual surveys were analysed using 'line transect' protocols and thermal imaging as 'points', each assuming 360° field-of-view. Camera trap surveys were also analysed as points; however survey effort had a restricted 42° field-of-view of each camera, thus distance analysis for camera trap data multiplied total effort 'k' by 42/360 following Howe et al. (2017). Model fit was optimised in each case using truncation of the most distant detections and variable bin width as appropriate. Models assessed included uniform, half-normal and hazard-rate models; and model averaging was also considered. Models were evaluated by referring to Akaike information criterion (AIC), χ^2 goodness-of-fit test values, detection probability (P) values and coefficient of variation (P CV) using established methods (Buckland et al.

2001). As sequences of camera trap detections occurring over several seconds were not independent we calculated the overdispersion factor ($\hat{C}$) and used log likelihood ($\mathcal{L}$) to calculate QAIC, i.e. the two step model evaluation approach of Howe et al. (2018).

Statistical analysis

Descriptive statistics were tabulated for a suite of parameters capturing survey effort, numbers of detections, detection distances and encounter rates for each survey method. Based on the surveys' efforts and results, we calculated and compared the level of effort to achieve a required precision of density estimate, using formulae from Buckland et al. (2001). Spatial autocorrelation of sightings (encounters) was examined with kernel density maps of detections using ArcGIS ver. 10.6.1 and tested using Moran's I index for each survey method. Comparison of sighting densities between the three methods was assessed by Pearson correlation of the kernel density maps. ArcGIS was used to map topographical gullies plotted as shapefile vector data (Ordnance Survey 2018), converted into a raster of gully density using the line density and polygon to raster toolbox functions (100 m cell size). The relationship between hare encounter rates and gully density was examined using linear regression for each survey method. Temporal trends in camera trap encounter rate were examined using a separate general linear mixed model (GLMM) fitting 'Site' as a random factor to account for multiple observations per site (multiple days recording) and the sequential deployment of cameras at different sites, and with 'days since start of survey' fitted as fixed effect. Daily detections followed a negative binomial distribution. Statistical analyses were conducted using R ver. 3.6.1 (<www.r-project.org>) and R-package 'lme4' (Bates et al. 2015) for linear models following Crawley (2002).

Results

Daylight visual surveys

Over five days, the six sites were surveyed for a total of 26 h (Table 1, Supporting information). Daylight visual line transect surveys required 3–7 h per transect which were 4–8 km in length. Mean radial detection distance was 152 m and the furthest was 532 m. Thus, the survey rate was 0.98 km² per hour (Table 1). In total, 41 mountain hare detections were recorded with 1 detection every 0.63 h (~38 min). During daylight hours 95% of the detections were of solitary individuals, the remainder being pairs (Table 1). Owing to hiding and flushing behaviour of hares, 16 detections occurred within 30 m of the observer. Thus to enable a choice of detection function models, we truncated data at 100 m and assigned observations to bins at 5, 10, 20 and 100 m (Table 2). Candidate models showed high χ^2 goodness-of-fit (GOF) values (> 0.31) with similar detection probabilities. The half-normal model reported lowest AIC, p = 0.28, (cv) = 0.20 and was selected for density estimation. (Table 2, Fig. 3a). Following data truncation, encounter rate was 0.82 km⁻¹, (cv) = 0.31 and observations were singles making

Table 1. Descriptive summary of sampling effort, detections and their distance from the observer and surveyed area (based on furthest detection distance) for daylight visual surveys, thermal imaging and camera trapping. Samples and detections are total values before truncation. Per method 'Summary' rows: Σ=column total; $\bar{x}$ =column mean. All camera trap values based on night-time (informed by Fig. 4). Calculation of area surveyed at each site for cameras=(further detection distance per site)^2 × π × camera field of view restriction (42/360) × number of cameras per site. The survey rate (km^2 per hour) for camera traps is not calculated as they are considered to be in continual operation.

Method (survey units)	Samples	Hours effort	Detections	Mean cluster size	Mean detection distance (m)	Furthest detection (m)	Detections per hour	Hours to 1st detection	Surveyed area (km²)	Survey rate (km² per hour)
Daylight visual surveys Sample units=Transect length km										
Site 1	4.62	3	8	1.00	149	305	2.67	0.38	3.11	1.04
Site 2	4.82	4	11	1.09	220	446	2.75	0.36	4.92	1.23
Site 3	4.71	4	1	1.00	192	192	0.25	4.00	1.93	0.48
Site 4	4.70	4	12	1.08	172	532	3.00	0.33	5.89	1.47
Site 5	4.89	4	5	1.00	87	362	1.25	0.80	3.95	0.99
Site 6	8.16	7	4	1.00	94	263	0.57	1.75	4.51	0.64
Summary	Σ=31.91	Σ=26	Σ=41	$\bar{x}$ =1.03	$\bar{x}$ =152	$\bar{x}$ =350.0	$\bar{x}$ =1.75	$\bar{x}$ =0.63	Σ=24.31	$\bar{x}$ =0.98
Thermal imaging Sample units=points (number of replicates in brackets)										
Site 1	12 (20)	16	26	1.34	185	508	1.63	0.62	16.21	1.01
Site 2	12 (22)	22	38	1.31	256	612	1.73	0.58	25.88	1.18
Site 3	12 (27)	19	30	1.43	218	500	1.58	0.63	21.20	1.12
Site 4	12 (22)	20	87	1.44	270	682	4.35	0.23	32.14	1.61
Site 5	12 (12)	10	12	1.08	436	740	1.20	0.83	20.64	2.06
Site 6	11 (11)	10	13	1.38	220	528	1.30	0.77	9.63	0.96
Summary	Σ=71 (114)	Σ=97	Σ=206	$\bar{x}$ =1.33	$\bar{x}$ =264	$\bar{x}$ =595.0	$\bar{x}$ =1.96	$\bar{x}$ =0.47	Σ=125.71	$\bar{x}$ =1.32
Camera traps Sample units=number of cameras (total camera nights in brackets) [hours per night in square brackets]										
Site 1	16 (287) [17]	4879	768	1.00	2.33	9	0.15	6.35	0.000475	–
Site 2	16 (376) [17]	6392	550	1.00	2.60	10	0.08	11.62	0.000586	–
Site 3	12 (148) [16]	2368	213	1.00	1.92	6	0.09	11.12	0.000158	–
Site 4	16 (331) [15]	4965	1128	1.00	2.91	12	0.23	4.40	0.000844	–
Site 5	16 (386) [14]	5404	479	1.00	2.60	8	0.09	11.42	0.000375	–
Site 6	15 (272) [13]	3536	573	1.00	2.41	9	0.16	6.17	0.000445	–
Summary	Σ=91 (1800) [varying]	Σ=27 544	Σ=3705	$\bar{x}$ =1.00	$\bar{x}$ =2.46	$\bar{x}$ =9	$\bar{x}$ =0.13	$\bar{x}$ =8.51	Σ=0.002884	–

6

1.00 cluster size (Table 3). The contribution to variation of density estimate was encounter rate (72.5%) and detection probability (27.5%).

Night-time thermal imaging

Over eleven nights, a total of 114 point transects located along the boundary of the six sites were surveyed for a total of 97 h (Table 1, Supporting information). Surveys needed 5–7 h to cover up to 12 points per night. Mean detection distance was 264 m and the furthest was 740 m. Thus, the survey rate was 1.32 km² per hour or 0.00587 km² (i.e. 5870 m²) per point (Table 1). In total, 206 mountain hare detections were made with 1 detection every 0.47 h (~28 min). During darkness 74% of detections were solitary individuals, the remainder groups of up to 8 hares (Table 1). For modelling, detections were truncated at 350 m. All candidate detection functions achieved model fit (Table 2). The hazard-rate model had lowest AIC and highest χ^2 GOF = 0.78 with P = 0.34, (cv) = 0.21 and was selected for density estimation (Fig. 3b). Following data truncation encounter rate was 1.33 k⁻¹, (cv) = 0.12 and estimated cluster size 1.31, (cv) = 0.04 (Table 3). The contributors to variation of density estimate were encounter rate (24.5%), detection probability (73.9%), cluster size (1.6%).

Camera traps

Over four months, a total of 91 camera locations were installed throughout the six survey squares (total = 1800 days i.e. 27 544 night hours) (Table 1, Supporting information). In total, 107 000 images were captured, retrieving 5112 images of mountain hares per 1 second snapshot window. The remaining images were false triggers: wind-blown vegetation or other animals e.g. foxes, stoats *Mustela erminea*. Of these images 1329 showed hares attracted to marker canes or the camera, so were excluded, leaving 3783 separate detection events.

Of these, just 78 detections (2%) occurred by day; 3705 detections (98%) during night-time, averaging 1 detection per 8.5 h (Table 1). Night-time showed the largest activity peak after sunset, followed by moderate activity periods, and a distinct peak before dawn (Fig. 4). This pattern was similar at each site for the study duration: activity occurring over 17 night hours late November (site 1), compressing into 13 night hours late March (site 6). However the timing of night-time activity peaks differed between sites. The highest correlation was 86% between sites 1 and 5; the lowest correlation 51% between sites 3 and 6. Based on night-time detections, the mean detection distance was 2.4 m and the furthest was 12 m, and 95% of detections were within 5 m of the camera (Table 1). Thus, the survey rate averaged 0.0003 km² (i.e. 30.0 m²) per camera (Table 1). Night-time detections for distance analysis modelling assessments were allocated to bins at 1, 2, 3–4 and 5 m (Table 2). Having calculated QAIC and ($\hat{C}$) for candidate models, the latter was lowest for the hazard-rate model at 1.8 and χ^2 GOF = 0.18, thus was selected for reporting with P = 0.17, (cv) = 0.03 (Table 2 Fig. 3c). Camera trap encounter rate was 0.00030 k⁻¹, (cv) = 0.14 (Table 3, Supporting information). Cluster size was 1.00, (cv) = 0.01. The contribution of variation to the density estimate was encounter rate (95.4%) and detection probability (4.5%).

Table 2. Summary of models showing number of parameters (# para), AIC, Delta AIC, χ^2 values, degrees of freedom (df), and χ^2 goodness of fit (GOF), detection probability (P) and co-efficient of variation values (P CV). For camera traps, log likelihood (log $\mathcal{L}$), overdispersion factor ($\hat{C}$) and QAIC are shown for assessments of over-dispersed data (Howe et al. 2018). For each survey method, data selections and number of observations (n obs) are listed. Models selected for subsequent estimations are marked with asterisk *.

|	Model (key)	# para	AIC	Delta AIC	χ^2	df	χ^2 GOF	p	P CV	log $\mathcal{L}$	$\hat{C}$	QAIC
	Daylight visual surveys	Data truncation at 100, bins at 5 m, 10 m, 20 m and to 100 m, n obs = 26										
	Uniform + cos	2	74.3	2.3	0.7	1	0.40	0.31	0.36			
	Uniform + polynomial	1	72.3	0.3	0.6	2	0.73	0.30	0.18			
*	Half-normal + cosine	1	72.0	0.0	0.4	2	0.82	0.28	0.20			
	Half-normal + Hermite	1	72.0	0.0	0.4	2	0.82	0.28	0.20			
	Hazard-rate	2	74.6	2.6	1.0	1	0.31	0.33	0.15			
	Thermal Imager	Data truncation at 350 m, n obs = 152										
	Uniform + cosine	2	1753.6	0.9	11.2	15	0.73	0.29	0.13			
	Uniform + polynomial	3	1755.9	3.3	11.2	14	0.66	0.31	0.12			
	Half-normal + cosine	3	1753.9	1.3	9.7	14	0.77	0.32	0.29			
	Half-normal + Hermite	1	1757.7	5.0	17.6	16	0.34	0.38	0.09			
*	Hazard-rate	2	1752.6	0.0	10.5	15	0.78	0.34	0.21			
	Camera traps	Data truncation at 5 m, bins at 1, 2, 3–4, 5 m; n obs = 3506										
	Uniform + cosine	1	9371.4	875.2	876.4	2	0.00	0.30	0.01	−4684.6	438.2	12.9
	Uniform + cosine	2	8607.4	111.2	109.3	1	0.00	0.18	0.02	−4301.7	109.3	14.0
	Uniform + polynomial	1	10010.5	1514.3	1598.5	2	0.00	0.38	0.01	−5004.2	799.3	13.6
	Uniform + polynomial	2	9359.1	862.9	863.2	1	0.00	0.30	0.02	−4677.5	863.2	14.8
	Half-normal + cosine	1	8709.6	213.4	255.9	2	0.00	0.17	0.02	−4353.8	128.0	36.3
	Half-normal + cosine	2	8562.5	66.3	68.7	1	0.00	0.12	0.03	−4279.2	68.7	37.7
	Half-normal + Hermite	1	8709.6	213.4	255.9	2	0.00	0.17	0.02	−4353.8	128.0	36.3
	Half-normal + Hermite	2	8710.4	214.2	254.2	1	0.00	0.17	0.05	−4353.2	254.2	38.3
*	Hazard-rate + simple	2	8496.2	0.0	1.8	1	0.18	0.17	0.03	−4246.1	1.8	4721.9
	Hazard-rate + simple	3	8498.2	2.0	1.7	0	0.00	0.17	0.03	−4246.1	–	–
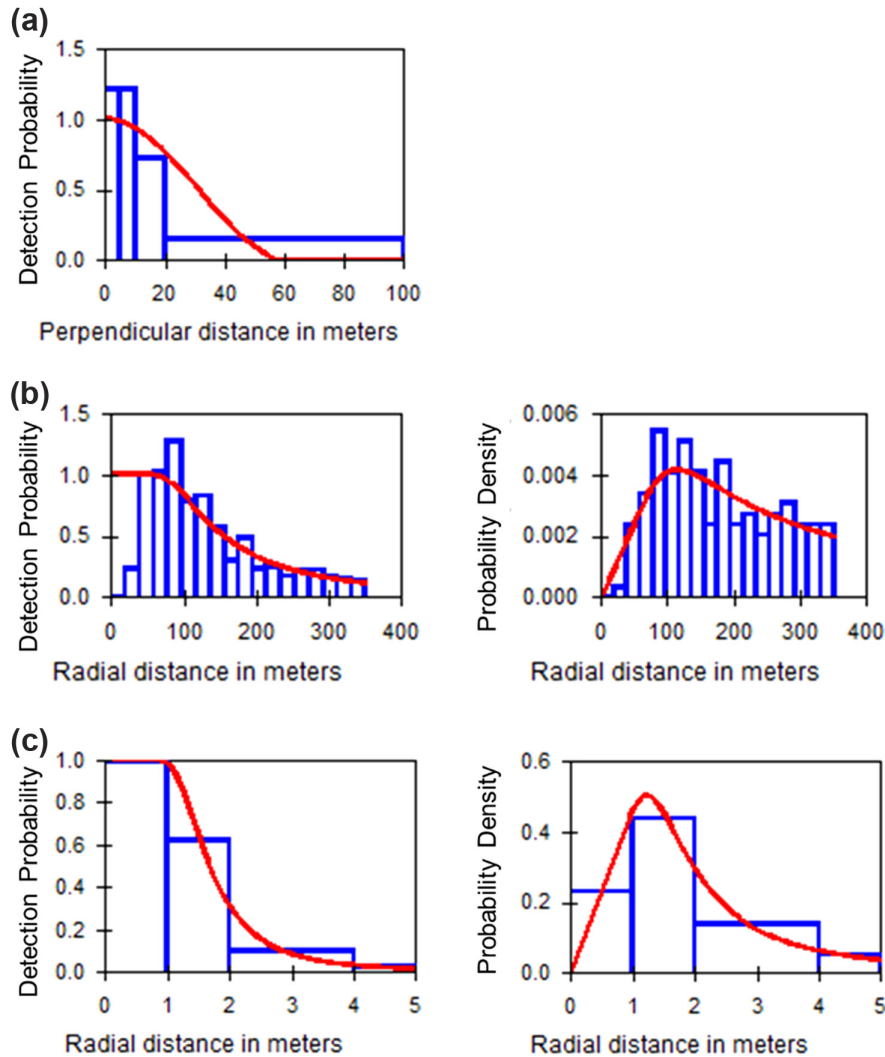
Figure 3. Distance sampling detection probability and probability density function histograms for (a) daylight visual surveys (uniform model with cosine adjustment and data allocated to bins at 5, 10, 20 and to 100 m), (b) nocturnal thermal imaging (hazard-rate model with simple polynomial adjustment and data truncated at 350 m), (c) camera traps (hazard-rate model with simple polynomial adjustment and data allocated to bins at 1, 2, 4 and to 5 m.

Comparison of methods

Distance sampling models from daylight visual surveys estimated density at 14.3 hares km^{-2} (95%CI 6.3–32.5). Night-time thermal imaging from points estimated density at 12.1 hares km^{-2} (95%CI 7.6–19.4). Camera trapping estimated density was 22.6 hares km^{-2} (95%CI 17.1–29.9) (Table 3).

Extrapolated to the entire 49 km^2 study site at Holme Moss, density estimates suggested a total population of 705 hares (95% CI 311–1597) from daylight visual surveys, 597 hares (95% CI 374–951) from thermal imaging and 1109 hares (95% CI 839–1467) from camera traps (Table 3).

Assessing the density estimates and the effort required to achieve reliable precision i.e. 20% coefficient of variation, daylight visual surveys would require 109 km of transects; thermal imagers would require 164 points; and camera traps would require 45 installations (Fig. 5). Comparing field effort daylight visual surveys surveying at 1.2 km per hour would require 89 h effort; thermal imager surveying 1.2 points per hour would need 140 h effort. Camera traps needing 3 h per installation (1 h set up, 1 h revisit, 1 h take down) would require 134 h of field effort and if a manual image review process was used (e.g. Timelapse software with auto-completing data entry, estimating 15 s per image), a further 218 h of desk time (Fig. 5).

Spatial and temporal variation

Considering sighting locations per site (untruncated data), daylight visual surveys showed large differences of sightings (encounter rates) with site 3 lowest at 0.2 km^{-1} and site 4 highest at 2.5 km^{-1}, with a sparse distribution except for sites 2 and 4 (Fig. 6). Thermal imager observations occurred at a mean rate from 1.0/point (site 5) to 3.9/point (site 4) (Fig. 6) and appeared to show 2 clumped distributions around site 4 (Fig. 6). Of the thermal imager points, 99 achieved detections, 15 did not, indicating mostly widespread presence of hares across all sites. Camera trap observations occurred at a mean rate from 0.0002 k^{-1} (site 3) to 0.0005 k^{-1} (site 4), and showed the most intense occurrence around site 4 (Fig. 6). Of the 91 cameras, 77 achieved detections and 14 made no detection, indicating a widespread distribution though with some negative locations.

8

Table 3. Estimates of detection probability, density and abundance obtained from distance sampling analyses for all three survey methods. Value=point estimate; CV=coefficient of variation; LCL and UCL 95% lower and upper confidence limits. Encounter rate: Daylight visual n/km=encounters per km; Thermal imager: n/k=encounters per point; Camera traps n/k=encounters per second. Abundance estimate derived from density value projected to the 49 km² of Holme Moss.

Method	Value	CV	LCL	UCL
Detection probability				
Daylight visual surveys	0.28	0.20	0.19	0.42
Thermal imager	0.34	0.21	0.23	0.50
Camera traps	0.17	0.03	0.16	0.18
Encounter rate				
Daylight visual surveys (n / km)	0.82	0.31	0.36	1.81
Thermal imager (n k)	1.33	0.12	1.05	1.68
Camera traps (n/k)	0.00030	0.14	0.00023	0.00039
Cluster size				
Daylight visual surveys	1.00			
Thermal imager	1.31	0.04	1.20	1.44
Camera traps	1.00	0.01	1.00	1.00
Effective strip or radius width (m)				
Daylight visual surveys	28.3	0.19	18.9	42.2
Thermal imager	202.5	0.10	165.3	248.2
Camera traps	2.1	0.01	2.00	2.13
Density (hares km^{-2})				
Daylight visual surveys	14.3	0.37	6.3	32.5
Thermal imager	12.1	0.24	7.6	19.4
Camera traps	22.6	0.14	17.1	29.9
Abundance				
Daylight visual surveys	705	0.37	311	1597
Thermal imager	597	0.24	374	951
Camera traps	1109	0.14	839	1467

Hare detections were not spatially autocorrelated using any survey method (Moran's $I_{daylight\ visual}=-0.12$, Z=0.12; Moran's $I_{thermal\ imaging}=0.07$, Z=0.99; Moran's $I_{camera\ traps}=-0.15$, Z=−0.27). Sighting density was strongly spatially correlated between the three methods (Pearson $r_{daylight\ visual\ \sim\ thermal\ imager}=0.55$, p < 0.001, $r_{thermal\ imager\ \sim\ camera\ traps}=0.45$, p < 0.001 and $r_{camera\ traps\ \sim\ daylight\ visual}=0.52$, p < 0.001 (Fig. 6 and Supporting information). Site 4 was consistently estimated to have the highest sighting density regardless of the survey method (Fig. 6). Sites 1 and 2 also had substantial sighting densities.

Site encounter rates using daylight visual surveys and camera trap surveys were unaffected by gully density but encounter rates using night-time thermal imaging were significantly negatively associated with gully density ($F_{1,4}=9.11$, β ± SE=−0.833 ± 0.0009, p=0.039, $r^2=0.69$). Site 4 which had the highest density estimate of mountain hares, had the lowest gully density of any site (Fig. 7).

Camera traps ran continuously (24/7) from November to March. Sequential deployment (accounted for imperfectly using the random factor of site) reported encounter rates showing a near significant decline by 62% over the four months from 37.6 to 14.3 encounters per day (Fixed effects standardised β=−0.009, z=−1.55, p=0.12; Random effects: Site Var=0.10 SD=0.324; Fig. 8).

Discussion

Our study compared three survey methods for mountain hares which provided very different kinds of observations and density estimates. Daylight visual surveys produced the fewest observations, seeing mainly single hares and appear-ing to under record many hares hiding by day. The method did provide sufficient observations to enable monitoring of relative density but with very wide confidence intervals. By night the thermal imager frequently observed single or large groups of hares over the furthest distances and estimated density with narrower confidence intervals. However thermal imaging opportunities were limited by bad weather. Camera traps monitored constantly and achieved the largest number of detections reflecting night time activity of hares, capturing mostly single animals at very short observation distances. Camera trap density estimates were much larger than for daylight visual sampling and thermal imaging and were more reliable, but were susceptible to many assumptions. Notwithstanding differences in detection rates the locations of sightings from each method were highly spatially correlated.

Daylight visual surveys

Daylight visual surveys for mountain hares have been criticised when used in areas of low density or during the day when hares are inactive (Petrovan et al. 2011, Newey et al. 2018). Our expectation was Holme Moss would elicit frequent occurrences of hares (Mallon et al. 2003), yet we achieved very few observations. The small sample size we achieved was below the minimum required for distance sampling and contained some heaping of detection distances. The nature of hiding and flushing hares caused many detections to occur at short range. Thus, when selecting detection function models, we were obliged to use a smaller data set with few, wide bins. This selection may have also precipitated a narrow effective strip width and this may have contributed to the overall density estimate as being higher
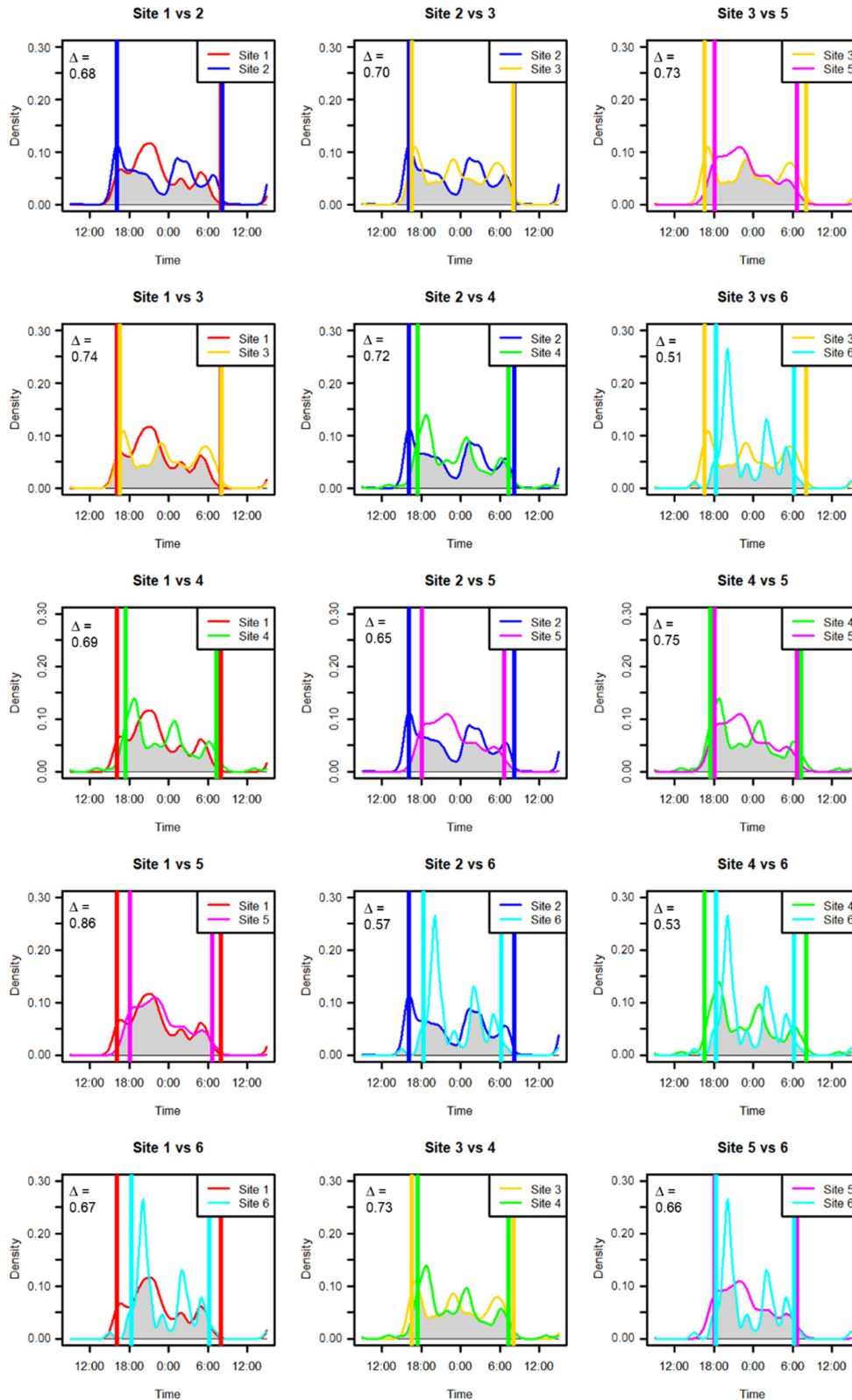
9

Figure 4. Diel activity at sites showing von Mises kernel densities and pairwise overlaps with other sites. The x-axis shows time of day. The y-axis is the frequency estimate of detections. The overlap of densities, common to each pair of sites, is the shaded grey area below both curves. Overlap coefficient values between compared densities is top left. The mean overlap of all pairwise combinations was 68%; all exceeded 50%. Vertical lines indicate sunrise and sunset times for each site pair; night-time hours reducing with spring onset. Dates of operation: site 1: 24 Nov 2017–18 Dec 2017 (17 night hours); site 2: 11 Dec 2017–11 Jan 2018 (17 night hours); site 3: 9 Jan 2018–25 Jan 2018 (16 night hours); site 4: 25 Jan 2018–9 Mar 2018 (15 night hours); site 5: 16 Feb 2018–30 Mar 2018 (14 night hours); site 6: 9 Mar 2018–30 Mar 2018 (13 night hours). Images produced with R-package 'overlap' (Meredith and Ridout 2020) based on Ridout and Linkie (2009).
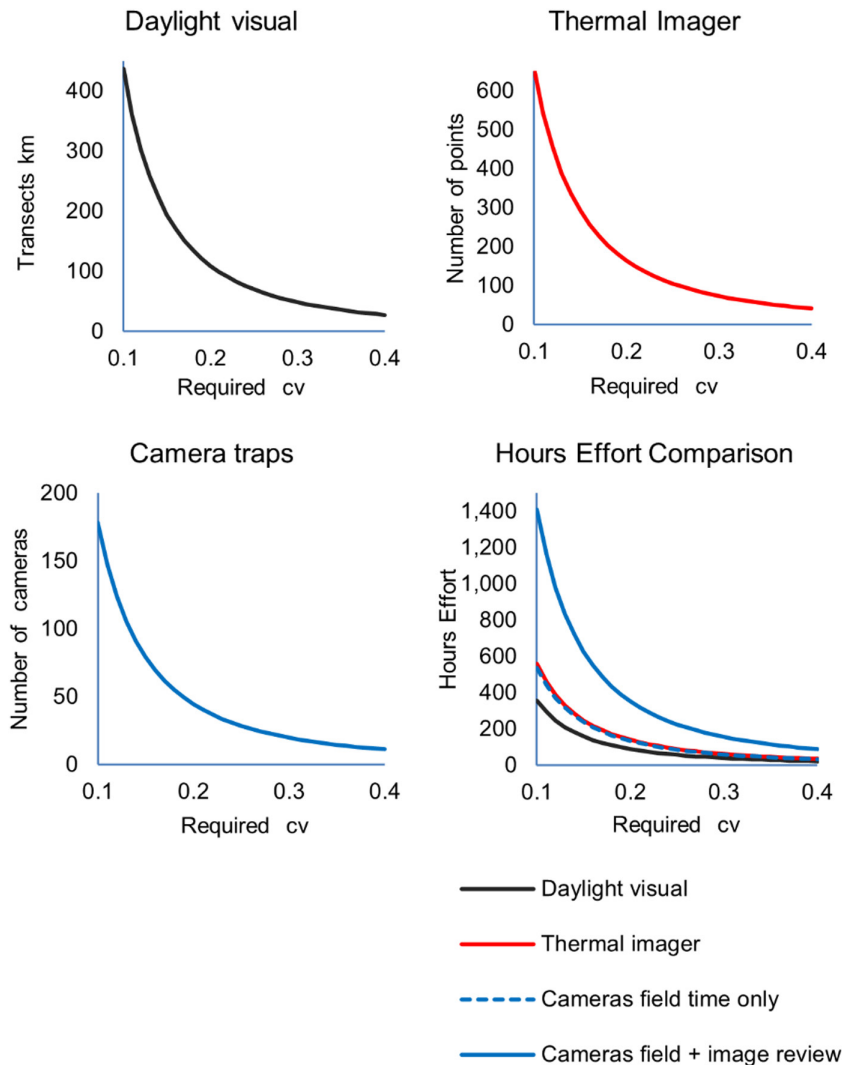
10

Figure 5. Effort required to achieve a target precision of density estimate, as measured by coefficient of variation. Input to the hours effort comparison is based on Table 1 and assumes for daylight visual surveys 1.2 km h⁻¹ walked; for thermal imagers 1.2 point h⁻¹ surveyed. Camera traps assumes cameras are in situ for average 21 days. 'Camera field time only' based on 3 h per camera being one installation visit, one maintenance visit, one retrieval visit. 'Image review' time assumes 1176 images per camera achieved with 15 s review time per image = additional 4.9 h per camera.

than for thermal imaging. This was surprising as one might expect thermal imaging to be observing more such nocturnal animals leading to a higher encounter rate and density estimate. Although detection probability variation was moderate, encounter rate variation was high. Consequently, the density estimate possessed wide confidence intervals and variation. To achieve reliable estimates, useful for ongoing monitoring, surveys should achieve 80 or more detections (Buckland et al. 2001). This suggests that studies similar to ours would benefit from replicate surveys to achieve a larger sample size to result in more accurate population density estimates, were this important for monitoring design goals. In retrospect for our own study we might have sacrificed some camera trap management time for more line transect surveys. Alternatively, daylight survey effectiveness might be improved by 3 or 4 observers walking abreast. Daylight visual surveys provided an advantage as transect routes forced the observer to traverse gullies, opening up fields of view and occasionally enabling sheltering hares to be seen.

Night-time thermal imaging

This study deployed an advanced thermal imager with mounted laser range finder for measuring distances to object in complete darkness and with point transect protocols. Whilst seemingly dangerous to walk across moorland by night, this could in fact be done as safely as by day, though slower. However, it was physically difficult to achieve 12 vantage points, spaced 333 m apart, in a single night for a single observer. As the thermal imager was viewed through two lenses on its internal screen, it provided a 3D image and alleviated issues of eye strain. Cold temperatures below −5°C flattened batteries within 60 min. Sinking hill fog or increasing winds through some nights, cut surveys short. Thermal imaging enabled observations of hares across a broad landscape, where they exhibited feeding and social behaviour. The presence of the observer did not prompt evasive movement. The method worked well on snow. Encounter rates provided a sample size greater than the ∼ 80 detections
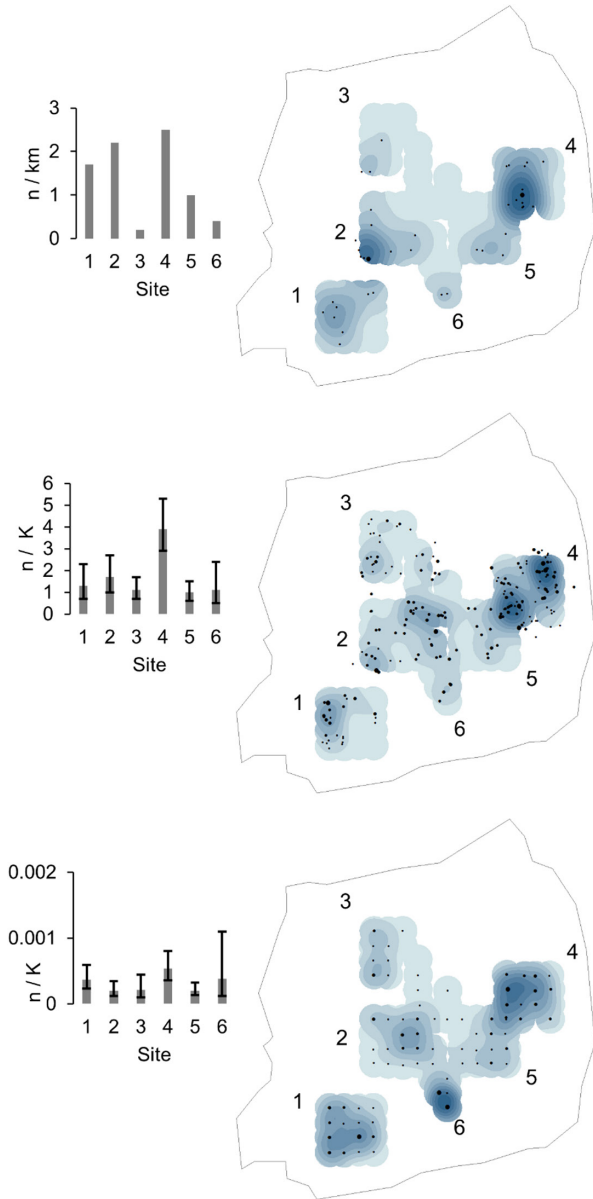
Figure 6. Sightings per method per site for (a) daylight visual surveys, (b) thermal imager and (c) camera traps. Column charts show encounter rate value estimates based on all sightings, with 95% confidence intervals for thermal imager and camera traps. Kernel density maps show spatial variation of hare sightings, with site numbers. Black dots indicate sightings, increasing in size to show clusters for daylight visual and thermal imager, (normalised for replicates) and camera traps (normalised for nights in operations). Background shading increases to dark based on sighting intensity. Kernel density boundaries are based on 333 m buffer of camera locations, hence some daylight visual sampling and thermal imager encounters fall outside this area.

required according to distance analysis standard guidelines (Buckland et al. 2001). Distance histograms showed good model fit: a broad shoulder and gradually decreasing distance shape, providing lower variation of detection probability. The lack of detections within 30 m might suggest evasive movement by hares, although this may be expected when carrying out distance sampling with point counts (Buckland et al. 2001). Rumpled terrain occasionally meant hares
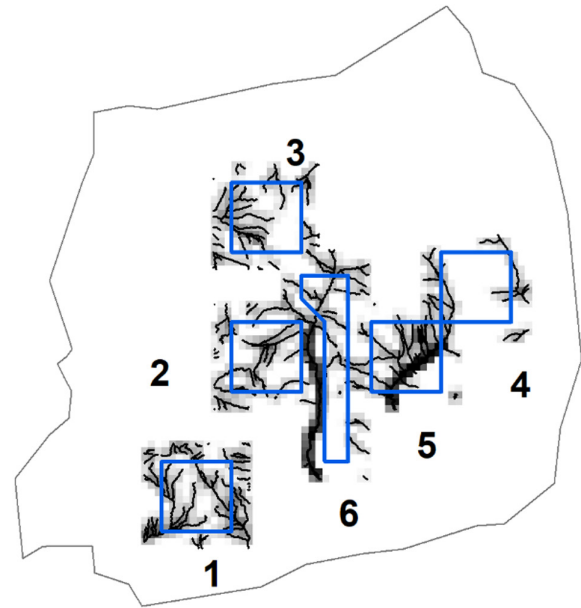

Figure 7. Map of gullies (lines) with gully density (cells) across the six study sites at Holme Moss. Numbers denote each study site.

might be within viewing range but hidden in gullies. Future thermal imaging studies could by day prospect for a large set of unimpeded vantage points, from which to draw a random sample to visit by night. Our findings suggested high levels of precision could be achieved with a logistically manageable number of points, requiring ~15 nights, assuming favourable weather. Such a device is a considerable investment.

Camera traps

Camera traps provided a practical method of constant surveillance in all weathers including snow. Installation of cameras across moorland was slow: often one day for two people to move four cameras, two kilometres. The 2–3 kg size of
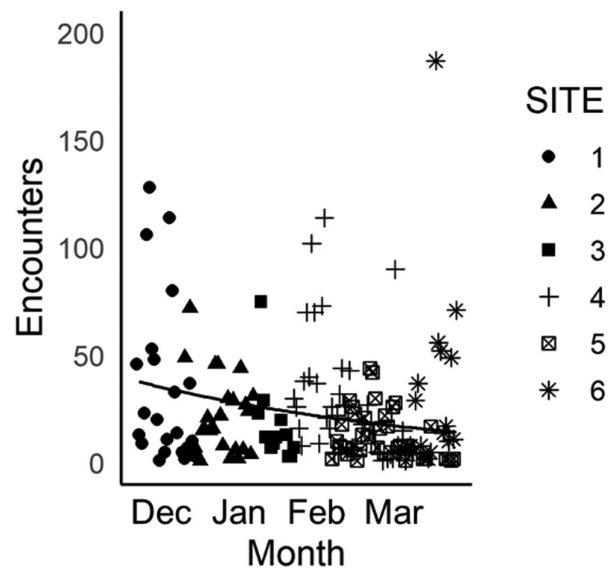

Figure 8. The regressed number of encounters (line) per camera (point shapes) is seen to decrease over the study period, end Nov 2017 to March 2018, taking into account 'Site' as a random effect.

12

hares required maximum camera sensitivity, also capturing blowing vegetation and 'blank' images, requiring more filtering time. However, operating 24/7, cameras appeared to avoid false negative detections. Image times conveyed peak nocturnal activity periods, even during extremely cold nights. There were two night-time peak activity phases, consistent with records for Irish hare *Lepus timidus hibernicus* Caravaggi et al. (2018). The narrow field of view captured no more than 2 hares at a time, perhaps under recording larger groups, as observed by the thermal imager. Camera traps require financial outlay, bear theft risk and need considerable field effort. Image review time is substantial yet can be reduced using image recognition software (Schneider et al. 2020).

In our study, camera trap detections occurred at short ranges, so the detection probability histogram allocated 3506 encounters to just four distance bins, producing low variation of detection probability (cv = 0.03). Camera trap density estimates showed less variation than the thermal imager. Our findings suggested high levels of precision could be achieved with half the camera installations as we had used, with field time of ~ 20 days.

Monitoring surveys are expected to fulfil the principal assumptions of distance sampling. However, for the camera trap analysis we noted certain factors can have a large effect on density estimates (Fig. 9).

Firstly, most of our camera trap detections occurred at very short distances ($\leq$ 5 m) creating a fine scale sensitivity in the detection function histogram for our Distance analysis. The low detection probability estimate (0.17), implied to 5 m, 83% of hare encounters were missed and reported a short effective strip radius (2.1 m), implying a higher density estimate. This radius was smaller than recorded elsewhere e.g. Hofmeester et al. (2016) at 3.69 m in dense understorey. This was surprising: when siting camera traps, we saw and avoided hare trails on snow and vegetation. However camera trap passive infra-red sensors can under-record at night, at different air temperatures, and micro-topography can affect detection rates (Hofmeester et al. 2018). It is possible detections may occur at further distances if surveying on flat arable-type land. Thus detection rates and measurement of lagomorphs in camera trap zones, merits further study within enclosure-based settings (Rowcliffe et al. 2008).

Secondly, snapshot window (k) definition greatly affected effort values and the number of defined detections. We opted for k = 1 second, which provided both the highest number of absolute encounters and also the most conservative estimate of encounter rate. Other studies have used
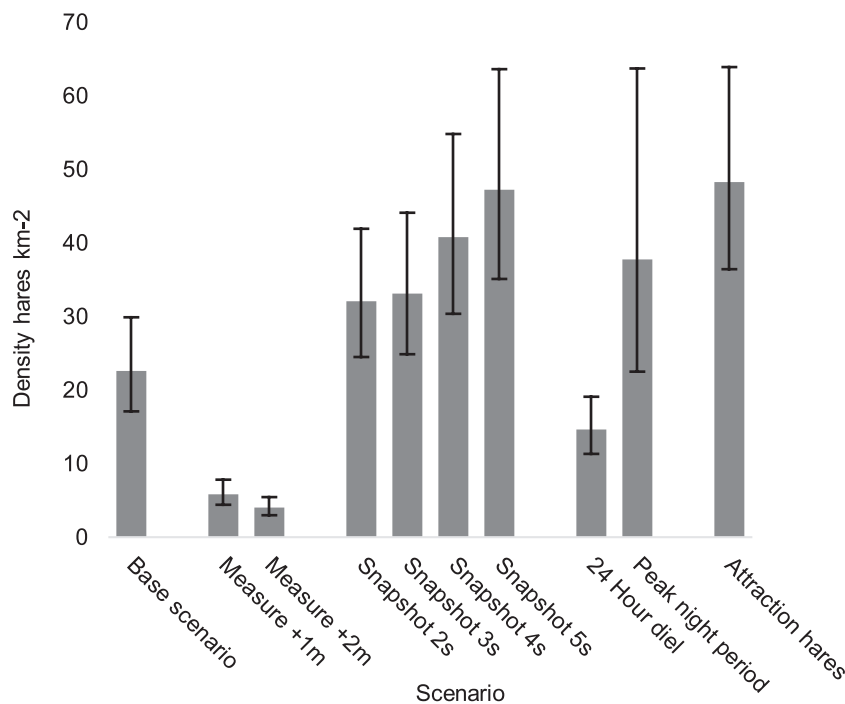

Figure 9. Analysis of alternate scenarios providing camera trap density estimates. The x-axis shows different data treatments or assumptions. The y-axis shows consequent density of hares km^{-2}. Columns are density values with 95% confidence interval error bars. To maintain consistency amidst the comparisons, all scenarios used the same data filter with detection distances binned at 1, 2, 4 and to 5 m with the Hazard-rate model with simple polynomial, which in all cases achieved lowest AIC scores of candidate models. 'Base scenario' was the scenario eventually chosen for our camera trap estimate for comparison with daylight visual sampling and thermal imager. This assumes correct measurements (metres) of distance to hare; k snapshot window = 1 second; diel period is sunset-to-sunrise (Fig. 4); and hare images showing attraction behaviour are discounted. The alternate scenarios each use the same assumptions and change one factor as follows: 'Measure +1 m, +2 m' highlights the effect of increasing the measured distance to camera of all hare detections by 1 m or 2 m which would lead to an increase in detection probability and lower density estimate. This is an exaggerated scenario, yet serves to demonstrate the sensitivity. 'Snapshot 2s, 3s, 4s or 5s' shows the effect of increasing snapshot window k, which reduces effort to a much greater degree than encounters, thus increasing density. '24 hour diel' uses full 24 hour period, correspondingly greater effort, very few additional detections. 'Peak night period' uses a 55% peak night activity period per site (McGowan et al. 2019) with consequently reduced effort. 'Attraction hares' includes a further 1318 images (after truncation) when dwelling behaviour observed.

longer durations: k = 2 seconds of Howe et al. (2017), k = 13 seconds (Corlatti et al. 2020). Our alternative scenarios suggested a gradual increase of k value brought fewer encounters, though disproportionate to the larger decrease in k units, thereby increasing encounter rates and thus density estimates. This effect diminished with increasing values of k. Further assessments of this relationship may require consideration of animal movement duration relative to camera detections, possible behavioural biases; or when modelling, setting thresholds for the influence of different values of k.

Thirdly, encounter rate estimation may be impacted by the number of night hours, varying by time of year and latitude or alternatively affected by choice of peak activity period (Frey et al. 2017, McGowan et al. 2019, Vazquez et al. 2019). Our activity frequency estimates showed different peak activity periods at different sites. This might have been caused by hares altering their feeding patterns because of changes to day length, or varying snow cover requiring longer foraging periods. Hence we chose sunset-to-sunrise for consistency between sites.

Fourthly, some images showed individual hares 'dwelling' on the camera trap site. Even with videos, it is hard to define such behaviour as happenstance or genuinely biased. A rules set may assist for rejecting such images. For example, we discarded any image where the hare's nose was within ~ 5 cm from the bamboo cane or camera. Attraction behaviour may be mitigated with marker canes used as reference photo, then removed, reprojecting their positions on ensuing computer images (Caravaggi et al. 2016), using video or having two cameras facing each other.

Ecological inferences

Between the methods we found a strong correlation between sighting density, and the similarity of detection probabilities for each method lend credibility to reported densities. The spatial correlation suggests the methods detected similar patterns of animal distribution even though they exhibited different detection rates. Methodological constraints (e.g. timing delay due to inclement weather) may explain some variation in our findings: some sites were surveyed early or late in the winter, during which time hare behaviour and consequent detectability changes. By late March, daytime hare activity often changes from dormant isolation to social grouping and mating. The assessment with the camera traps, statistically mitigating for site differences, showed encounter rates largely decreasing throughout the survey season. This may be understandable: an exceptional season of high winds and deep snow falls may have caused winter mortality.

These findings represent important indicative baselines for local monitoring and may inform assessments of other groups of native or reintroduced mountain hares. Notwithstanding its remarkable 150 year tenure, the Holme Moss mountain hare densities may be considered low compared to many populations in Scotland which commonly reach 20–50 hares km^{-2} (Watson et al. 1973, Newey et al. 2018).

Conclusions

We report the practical survey effort, scale, encounter rates, density estimates and measures of precision which may be helpful for the planning of studies of elusive or nocturnal animals in difficult terrain. Daylight visual sampling is low cost, is logistically simple, can rapidly cover much ground and can achieve precise density estimates, yet, transpiring by day, may fail to observe cryptic nocturnal animals, thereby reporting lower encounter rates and thus underestimating abundance. For somewhat more effort, a high power thermal imager achieves potentially more observations of nocturnal animals including at long distances and consequent higher density estimate precision. It is recommended when surveying accessible areas, with dependable fog and wind free weather. By contrast camera traps can provide constant monitoring and at night over long periods in all weathers. They are thus useful for long term surveys, placed in locations which are difficult to access frequently or where it would be hazardous to venture in darkness. Camera traps can achieve large numbers of detections, including at night, recording the peak activity levels of nocturnal animals.

However between the methods, daylight visual sampling and thermal imager surveys both work well in applying the principles of distance sampling. Practically speaking, camera trap distance sampling operates effectively in achieving large data sets and can adopt distance sampling principles. However the consequent models need contemplation of additional assumptions and sensitivity modelling. Where there is insufficient empirical data, inferences may require subjective analytical decisions, potentially rendering camera trap distance sampling estimations less robust.

Data availability statement

Data available from the Dryad Digital Repository: <http://dx.doi.org/10.5061/dryad.3r2280gg0> (Bedson et al. 2021).

References

Anderson, P. and Shimwell, L. 1981. Wild flowers and other plants of the Peak District. – Moorland Publishing.

Bates, D. et al. 2015. Fitting linear mixed-effects models using lme4. – J. Stat. Softw. 67: 1–48.

Bedson, C. P. E. et al. 2021. Data from: Estimating density of mountain hares using distance sampling: a comparison of daylight visual surveys, night-time thermal imaging and camera traps. – Dryad Digital Repository, <http://dx.doi.org/10.5061/dryad.3r2280gg0>.

Boulanger, J. and Krebs, C. J. 1994. Comparison of capture–recapture estimators of snowshoe hare populations. – Can. J. Zool. 72: 1800–1807.

Buckland, S. T. et al. 2001. Introduction to distance sampling. – Oxford Univ. Press.

Caravaggi, A. et al. 2016. An invasive–native mammalian species replacement process captured by camera trap survey random encounter models. – Remote Sens. Ecol. Conserv. 2: 45–58.

Caravaggi, A. et al. 2018. Seasonal and predator–prey effects on circadian activity of free-ranging mammals revealed by camera traps. – PeerJ 6: e5827.

Corlatti, L. et al. 2020. A field test of unconventional camera trap distance sampling to estimate abundance of marmot populations. – Wildl. Biol. 2020: wlb.00652.

Crawley, M. 2002. The R book. – Wiley & Sons.

DeMay, S. M. et al. 2013. Evaluating DNA degradation rates in faecal pellets of the endangered pygmy rabbit. – Mol. Ecol. Resour. 13 : 654–662.

Dingerkus, S. K. and Montgomery, W. I. 2002. A review of the status and decline in abundance of the Irish Hare *Lepus timidus hibernicus* in Northern Ireland. – Mammal Rev. 32: 1–11.

Frey, S. et al. 2017. Investigating animal activity patterns and temporal niche partitioning using camera-trap data: challenges and opportunities. – Remote Sens. Ecol. Conserv. 3: 123–132.

Harris, S. and Yalden, D. W. 2008. Mammals of the British isles: handbook, 4th edn. – The Mammal Society.

Harrison, A. K. 2011. Dispersal and compensatory population dynamics in a harvested mammal. – PhD thesis, Univ. of Glasgow.

Havens, K. J. and Sharp, E. J. 2016. Thermal imaging techniques to survey and monitor animals in the wild. – Elsevier Academic Press.

Hewson, R. and Hinge, M. D. C. 1990. Characteristics of the home range of mountain hares *Lepus timidus*. – J. Appl. Ecol. 27: 651–666.

HM Nautical Almanac Office. 2019. HM nautical almanac office: on-line data. – <http://astro.ukho.gov.uk/nao/online/>, accessed 2 April 2021.

Hofmeester, T. R. et al. 2018. Framing pictures: a conceptual framework to identify and correct for biases in detection probability of camera traps enabling multi-species comparison. – Ecol. Evol. 2019: 2320–2336.

Hofmeester, T. R. et al. 2016. A simple method for estimating the effective detection distance of camera traps. – Remote Sens. Ecol. Conserv. 3: 81–89.

Howe, E. J. et al. 2017. Distance sampling with camera traps. – Methods Ecol. Evol. 8: 1558–1565.

Howe, E. J. et al. 2018 Model selection with overdispersed distance sampling data. – Methods Ecol. Evol. 10: 38–47.

Hulbert, I. A. R. et al. 1996. Home-range sizes in a stratified landscape of two lagomorphs with different feeding strategies. – J. Appl. Ecol. 33: 1479–1488.

Krebs, C. J. 1989. The message of ecology. – Harper and Row.

Mallon, D. et al. 2003. Mountain hares in the Peak District. – Brit. Wildl. 15: 110–116.

McGowan, N. et al. 2019. National hare survey and population assessment 2017–2019. (Irish Wildlife Manual; Vol. 113). – National Parks & Wildlife Service.

Meredith, M. and Ridout, M. 2020. overlap: estimates of coefficient of overlapping for animal activity patterns. – R package ver 0.3.3. <https://CRAN.R-project.org/package=overlap>.

Newey, S. et al. 2003. Can distance sampling and dung plots be used to assess the density of mountain hares *Lepus timidus*? – Wildl. Biol. 9: 185–192.

Newey, S. et al. 2011. Development of a reliable method for estimating mountain hare numbers. – Scottish Natural Heritage Commissioned Report No. 444.

Newey, S. et al. 2018. Developing a counting methodology for mountain hares *Lepus timidus* in Scotland. – Scottish Natural Heritage Research Report No. 1022.

Ordnance Survey 2015. Explorer Map 1 Peak District. – Ordnance Survey, Southampton.

Ordnance Survey 2018. VectorMapLocal scale 1:10 000, tiles: SK, SE Updated: 1 July 2018, Ordnance Survey (GB), sourced using: EDINA Digimap Ordnance Survey Service. – <https://digimap.edina.ac.uk>, downloaded 28 February 2019.

Petrovan, S. O. et al. 2011 Detectability counts when assessing populations for biodiversity targets. – PLoS One 6: e24206.

Rao, S. J. et al. 2003. The effect of establishing native woodland on habitat selection and ranging of moorland mountain hares *Lepus timidus*, a flexible forager. – J. Zool. 260: 1–9.

Reid, N. and Montgomery, W. I. 2010. Retrospective analysis of the Northern Ireland Irish hare Survey data from 2002 to 2010. – Natural Heritage Research Partnership, Quercus, Queen's Univ. Belfast Northern Ireland Environment Agency Research and Development Series No. 11/16.

Reid, N. et al. 2007. Status of hares in Ireland. Irish Wildlife Manuals, No. 30. – National Parks and Wildlife Service, Dept of Environment, Heritage and Local Government, Dublin.

Ridout, M. and Linkie, M. 2009. Estimating overlap of daily activity patterns from camera trap data. – J. Agric. Biol. Environ. Stat. 14: 322–337.

Rowcliffe, J. M. 2014. Quantifying levels of animal activity using camera trap data. – Methods Ecol. Evol. 5: 1170–1179.

Rowcliffe, J. M. et al. 2008. Estimating animal density using camera traps without the need for individual recognition. – J. Appl. Ecol. 45 : 1228–1236.

Schneider, S. et al. 2020. Three critical factors affecting automated image species recognition performance for camera traps. – Ecol. Evol. 10: 3503–3517.

Sollman, R. 2018. A gentle introduction to camera-trap analysis. – Afr. J. Ecol. 56: 740–749.

Stubbs, F. J. 1929 The Alpine hare on the Pennines. – The Naturalist.

Sutherland, W. J. 2006. Ecological census techniques. – Cambridge Univ. Press.

Tallis, J. H. 1987. Fire and flood at holme moss: erosion processes in an upland blanket mire. – J. Ecol. 75: 1099–1129.

Thomas, L. et al. 2010. Distance software: design and analysis of distance sampling surveys for estimating population size. – J. Appl. Ecol. 47: 5–14.

TIMELAPSE 2 User Guide 2019. Saul Greenberg. – Univ. of Calgary, Canada.

UK Met Office 2019. – Met Office, Exeter, <www.metoffice.gov.uk/pub/data/weather/uk/climate/stationdata/sheffielddata.txt>, accessed January 2019.

Vazquez, C. et al. 2019. Comparing diel activity patterns of wildlife across latitudes and seasons: time transformations using day length. – Methods Ecol. Evol. 10: 2057–2066.

Watson, A. et al. 1973. Population densities of mountain hares compared with red grouse on Scottish moors. – Oikos 24: 225–230.

Yalden, D. W. 1971. The mountain hare (*Lepus timidus* L.) in the Peak District. The Naturalist No 918, pp. 81–92. – Yorkshire Naturalists' Union.